Proceedings of the
44th IEEE Conference on Decision and Control, and
the European Control Conference 2005
Seville, Spain, December 12-15, 2005

A Differential Model of the Baroreflex Control of the Cardiovascular System During a Tilt Test

Karima Djabella, Claire Médigue and Michel Sorine

Abstract— **In this paper, a differential model of the cardiovascular system and its baroreflex control is presented. This simplified model of the circulation includes the left heart, arterial and venous compartments, the afferent baroreceptor pathway, the sympathetic and vagal efferent activities and excitation-contraction coupling at the cardiac muscle level. The model is used to simulate the interactions among the baroreflex control loop, the pulsating heart and the effector during a graded orthostatic tilt. There is a satisfactory agreement between the model and experimental results illustrated through heart rate variability analysis. Experimental data on heart rate control can then be explained fairly well by a rather simple action of the sympathetic-parasympathetic system on the heart rate. The output of the proposed model are usually measured cardiovascular signals. An objective is to use it in model-based signal processing in order to assess the short-term control of cardiovascular system.**

I. INTRODUCTION

The cardiovascular system (CVS) is a complex mechanical, chemical, and hemodynamic system in which the variables are interrelated through a variety of feedback mechanisms. Among these mechanisms controlling the cardiovascular function, the most thoroughly investigated is the short-term control: the baroreceptor reflex system [1], [2].

Many mathematical models have been proposed to represent the dynamic regimes of the CVS in interaction with the baroreflex control loop [3], [4], [5]. In this study, we present a mathematical model of the CVS controlled by the autonomic nervous system (ANS). Compared with previous models, here the CVS and the ANS functions are both modelled by taking into account the major elements of their structures. By doing so, we gain physiological meaning for the model parameters but the closed loop behavior is now only indirectly modelled: we have to adapt the interface between CVS and ANS sub-models and to tune the ANS action (the control) in order to recover correct closed loop behaviors. The tilt test is used to assess the resulting model.

The model of the CVS is taken with minor changes from [6], where a differential model of the electro-mechanical activity of the cardiac muscle, first presented in [7], [8], is used coupled with windkessel models of the vascular compartments.

The complex structure of the multi-feedback baroreflex system, its function, and the role played by the different mechanisms have been the subject of a multitude of experimental studies in the last decades. These studies provide quite a complete description of the different components in both dynamic and static conditions. Nevertheless, understanding the behavior of the baroreflex system as a whole is still a hard problem, which is not yet completely resolved [5]. Many authors consider that the control objective is the heart rate itself and propose direct models for its regulation [9]. These ANS models suppose a constant stroke volume, so that controlling the heart rate is equivalent to control the blood flow averaged on a heart beat, which is the main cardiac function. Here, our stroke volume depends upon the pre-load and after-load conditions of the heart and we consider that the short term control objective of the ANS is the averaged blood flow regulation under arterial pressure constraints. In order to take into account the baroreflex loop in CVS modelling, several mathematical models have been proposed for the baroreceptor [10] and the ANS, for which we choose the model proposed in [2], that appears as a good basis to build a sound controller for the CVS.

The heart rate power spectrum exhibits a peak in low frequencies (LF) band (0.04-0.15 Hz) believed to be due to the baroreceptor mediated blood flow and pressure control and includes contribution from both the sympathetic and parasympathetic nervous system [3]. The aim of this paper is to show that our model is able to recover such heart rate variability during a tilt test.

The present article is structured as follows. First, a qualitative and quantitative description of the model is presented and parameter values are assigned. Subsequently, the model is validated by simulating experimental results concerning the interactions among the heart, pressure pulsatility and the baroreflex in normal closed-loop conditions. Finally, the system is simulated after a hemodynamic perturbation due to the transition from supine to standing posture (tilt test), to clarify the relative role of each mechanism in response to decrease of venous return to the heart.

II. MODEL DESCRIPTION

We model the heart as a controlled pump with variable pre-load and after-load conditions represented by two vascular compartments, systemic and venous. A detailed baroreflex loop is presented. Parameter assignments are given in tables I and II.

A. The Heart as a Pump

We have considered the left ventricle alone in a simple circulation circuit, see Figure 1. The contractile activity of the left ventricle is described, as for an isolated muscle fibre,

The authors are with INRIA-Rocquencourt, B.P. 105, 78153 Le Chesnay Cedex, France. Karima.Djabella, Claire.Medigue, Michel.Sorine@inria.fr

0-7803-9568-9/05/$20.00 ©2005 IEEE

by a three-element Hill-Maxwell model composed of a contractile element (CE) in series with an elastic element (SE), the series being connected in parallel with a passive element (PE). CE is under the control of a chemical input u, mainly depending on the calcium concentration. The following set of controlled differential equations is a constitutive relation, of visco-elasto-plastic type, between the stress σ_c and the strain ε_c in CE: [7], [8]:

$$\begin{cases} \dot{k}_c = -(|u| + \mu(\varepsilon_c) + \lambda|\dot{\varepsilon}_c|)k_c + k_0|u|_+ \\ \dot{\tau}_c = -(|u| + \mu(\varepsilon_c) + \lambda|\dot{\varepsilon}_c|)\tau_c + k_c\dot{\varepsilon}_c + \tau_0|u|_+ \\ \sigma_c = d_c(\varepsilon)(\tau_c + k_c\xi_0) + \eta_c\dot{\varepsilon}_c \end{cases} \quad (1)$$

where (the subscript c is used for CE variables):
- k_c is the stiffness, sometimes called variable elastance, proportional to the number of bound actin-myosin bridges.
- τ_c is the stress resulting from the actual stiffness and the internal deformation of the sarcomere.
- $u > 0$ controls the contraction and $u = 0$ (resp. $u < 0$) the passive (resp. active) relaxation and $|u|_+ = 1/2(u + |u|)$.
- $\mu(\varepsilon_c) = \mu^*(1 - k(\varepsilon_c - \varepsilon_{c0})^{1.6})$ is the contribution of elongation on the frequency at which cross-bridges unfasten [11].
- $d_c(\varepsilon) = (1+\varepsilon)^2$ is the density of possible actin-myosin bridges as a function of the total strain ε of the muscle.

The balance of forces between SE and CE, taking into account an acceleration of moving mass, leads to:

$$\mu_c\ddot{\varepsilon}_c = k_s(\varepsilon - \kappa\varepsilon_c) - \sigma_c \quad (2)$$

An exponential stress/strain relation is used to model PE:

$$\sigma_p(\varepsilon) = \frac{k_{p2}}{k_{p1}}\left(e^{k_{p1}\varepsilon} - 1\right) \quad (3)$$

The total stress σ can now be defined as a function of ε and u by using (1), (2) as the state equations for the muscle state variables ε_c, $\dot{\varepsilon}_c$, k_c, τ_c

$$\sigma(\varepsilon, u) = \sigma_p(\varepsilon) + \sigma_c \quad (4)$$

The isometric phase ($\dot{\varepsilon} = 0$), corresponding here to the isovolumic phase, is important in clinical applications to assess the heart contractility or to understand the interplay of extrinsic and intrinsic feedback controls (e.g. ANS action and Starling effect). The asymptotic value of σ in that case ($\dot{\varepsilon} = \dot{k}_c = \dot{\tau}_c = \dot{\varepsilon}_c = \ddot{\varepsilon}_c = 0$) is enlightening because, taking u as a function of the intracellular calcium concentration, it shows important control effects described, e.g. in [12]:

$$\sigma_{\mathtt{iso}}(\varepsilon, u) = \sigma_p(\varepsilon) + d(\varepsilon)\frac{(\tau_0 + k_0\xi_0)|u|_+}{\mu(\varepsilon) + |u|} \quad (5)$$

For contractions ($u(t) > 0$), we recover the Starling effect (σ increases with ε) through d and μ, the increasing of calcium sensitivity with ε through μ, the saturation of the control with the Hill-function shape of (5) with respect to u.

B. The Vascular Compartments

The simplified vascular system includes the left ventricle and two compartments, as shown in figure 1. This will be sufficient to take into account the effects of variable filling or ejection conditions. Blood flows from the venous compartment into the ventricle through the mitral valve, mimicked as an ideal unidirectional valve in series with a constant resistance. The blood is ejected from the left ventricle into the arterial compartment through the aortic valve.

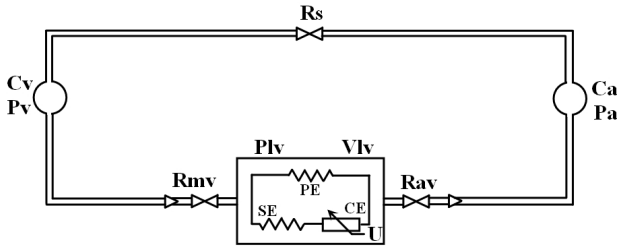

Fig. 1. Simplified hydraulic analog of the cardiovascular system.

In order to link the strain ε and stress σ in the muscle to the left ventricle volume V_{lv} and pressure P_{lv}, the ventricle is modelled as an incompressible cylinder of constant height and variable radius r and thickness e. Simple geometric considerations and Laplace's law show that:

$$\varepsilon = \sqrt{\frac{V_{lv}}{\bar{V}_{lv}}} - 1, \qquad P_{lv} = \left(\left(1 + \frac{V_m}{V_{lv}}\right)^{1/2} - 1\right)\sigma(\varepsilon, u) \quad (6)$$

The conservation of mass for the left ventricle leads to:

$$\dot{V}_{lv} = \frac{1}{R_{mv}}|P_v - P_{lv}|_+ - \frac{1}{R_{av}}|P_{lv} - P_a|_+ \quad (7)$$

where P_v and P_a are the venous and the arterial pressures.

The compartments are connected by capillaries and arterioles, modelled as a resistance R_s. They are characterized by their compliances C_a, C_v, such that their volumes are $V_a = C_a.P_a$ with C_a constant and $V_v = C_v(P_v).(P_v - P_{\mathtt{biasv}})$ where $P_{\mathtt{biasv}}$ is an external pressure representing orthostatic stress. Their models are the equations of conservation of mass. For the arterial compartment it is:

$$C_a\dot{P}_a = \frac{1}{R_{av}}|P_{lv} - P_a|_+ - \frac{1}{R_s}(P_a - P_v) \quad (8)$$

By assuming that the total amount of blood, V_t contained in the cardiovascular system is constant, we have:

$$C_v(P_v).\tilde{P}_v = V_t - C_aP_a - V_{lv}, \ \mathtt{with}\ \tilde{P}_v = P_v - \rho g h_v \sin\theta \quad (9)$$

In (9) θ is the angle of the graded tilt test and h_v is the distance to the hydrostatic indifference point, where we suppose that the pressure is regulated [13].

C. The Baroreflex loop

When the baroreflex loop is described (see figure 2), a distinction is made among the afferent pathway (involving the carotid baroreceptors and sinus nerve) and the efferent sympathetic and parasympathetic pathways [6].

Afferent pathway. The dynamic relationship between intrasinus pressure and the activity of the sinus nerve is described according to experimental results reported in the physiological literature [14]. Two main aspects arising from

TABLE I

CARDIOVASCULAR SYSTEM PARAMETERS

Left Ventricle		
passive relaxation parameter	λ	10
maximal stiffness	k_0	7500 $mmHg$
maximal stress	τ_0	500 $mmHg$
viscous friction coefficient	η_c	5247 $mmHg.s$
muscle volume	V_m	$3.15\bar{V}_{lv}$
stiffness of SE	k_s	30000 $mmHg$
% of CE in the SE-CE series	κ	61.25
inertia factor	μ_c	15 $s^2.mmHg$
growth factor of PE stiffness	k_{p1}	2
stiffness of PE for small strains	k_{p2}	7 $mmHg$
direct stress factor	ξ_0	0.1
relaxation rate parameter	k	0.4035 $1/\mu m$
relaxation rate parameter	ε_{c0}	1 μm
relaxation rate parameter	μ^*	25 $1/s$
Vascular System		
systemic resistance	R_{s0}	1 $mmHg.s/ml$
resistance sensitivity to control	k_{R_s}	1 $mmHg.s/ml$
venous compliance	C_{v0}	400 $ml/mmHg$
compliance sensitivity to control	k_{C_v}	0.5 $ml/mmHg$
compliance sensitivity to pressure	c_v	0.017 $ml/mmHg^2$
arterial compliance	C_a	2 $ml/mmHg$
aortic valve resistance	R_{av}	0.02 $mmHg.s/ml$
mitral valve resistance	R_{mv}	0.01 $mmHg.s/$ml
total volume	V_t	5000 ml
ventricle reference volume	$\tilde{V}_{lv}$	20 ml
initial venous volume	V_{iv}	$80\%V_t$
initial arterial volume	V_{ia}	$17.6\%V_t$
initial left ventricle volume	V_{ilv}	$2.4\%V_t$
initial venous pressure	P_{iv}	10 $mmHg$
initial arterial pressure	P_{ia}	90 $mmHg$

these experiments are considered. First, the relationship between intrasinus pressure and sinus nerve activity in static conditions exhibits a sigmoidal shape with upper saturation and lower threshold. Second, the carotid sinus baroreceptors are sensitive not only to the intrasinus pressure mean value but also to its rate of change [5]. In baroreceptor-heart rate studies in man however, one never assumes the detailed arterial pressure wave as input stimulus for the pressure receptors. It appears from the literature that there is a little consensus about what pressure should be considered as the most appropriate baroreceptor input. In continuous time models, the natural choice is the continuous arterial pressure as in [2]. In order to describe the response of the baroreceptor activity v_b to the arterial pressure, we use the simple equation originally proposed by [15]:

$$v_b = k_m\left[\tilde{P}_a - P_0\right] + k_d\dot{\tilde{P}}_a,\ \texttt{with}\ \tilde{P}_a = P_a - \rho g h_a \sin\theta \quad (10)$$

In (10) a bias depending upon θ modifies the measured pressure: it is the hydrostatic difference of pressure between the baroreceptor position and the hydrostatic indifference point, at the distance h_a.

A sigmoidal function represents the saturation and threshold characteristics of the baroreceptor response [16].

$$\overline{v_b}(t) = a\left[\arctan\left(\frac{v_b(t) - v_{b0}}{g}\right) + \frac{\pi}{2}\right] \quad (11)$$

Efferent sympathetic and parasympathetic pathways. The heart is influenced by the ANS in order to react to different stress situations. Three main effects are distinguished: the sympathovagal balance of the frequency of the sinus node, the contractility of heart, and the velocity of atrioventricular conduction (this last effect has not been taken into account because the atrium has not been considered). The sympathetic control dynamics N_s (of the three effectors: heart rate, peripheral resistance and compliance, and cardiac contractility) and the parasympathetic control dynamics N_v (of the heart rate) have been implemented as first order low-pass filters with pure time delays [17] .

$$\begin{cases} \tau_s\dot{N}_s(t) + N_s(t) & = \delta_s - K_s\overline{v_b}(t-\theta_s) \\ \\ \tau_v\dot{N}_v(t) + N_v(t) & = \delta_v + K_v\overline{v_b}(t-\theta_v) \end{cases} \quad (12)$$

The presence of pure delays in the responses is largely documented in the literature [3]; moreover, delays play a pivotal role in affecting the stability margin of the overall system and might be involved in the generation of Mayer waves. Both the sympathetic and parasympathetic components affect the heart rate $HR(t)$ which increases proportionally to vagal stimulation and decreases proportionally to sympathetic stimulation . The final heart rate level is then computed by multiplying the positive changes induced by the vagal stimulation, the negative changes induced by the sympathetic stimulation, and a constant level representing heart rate in the absence of cardiac innervation[17], [18].

$$HR = HR_0\left[1 + N_s\right]\left[1 - N_v\right] \quad (13)$$

The contractility I is not easy to model and not completely understood and evaluated,i.e., the contractility of the heart is extremely influenced by sympathetic nerves. The simplest choice is an additive first order low-pass filter with a time

TABLE II

BASAL VALUES OF BAROREFLEX LOOP PARAMETERS

Baroreceptor activity $\overline{v_b}$		
P_0	50	$mmHg$
k_m	0.01	$1/mmHg$
k_d	0.0025	$s/mmHg$
v_{b0}	1.0625	
a	0.2	
g	0.0001	
Sympathetic activity N_s		
τ_s	4	s
θ_s	2	s
δ_s	0.34	
K_s	1.00	
Vagal activity N_v		
τ_v	1.0	s
θ_v	0.5	s
δ_v	0.17	
K_v	0.55	
Contractility I		
τ_s^I	10	s
θ_s^I	2	s
δ_s^I	0.6	
K_s^I	1.3	
Heart rate HR		
HR_0	95	bpm

constant and a pure time delay that modulate a baseline inotropic condition, an augmentation of the baroreceptor activity causes a diminution of inotropic effect I.

$$\tau_s^I \dot{I} + I = 1 + \delta_s^I - K_s^I \overline{v_b}(t - \theta_s^I) \tag{14}$$

Among the observed control effects, there are a sympathetic vasoconstriction activation and a passive vasodilatation by inhibition of the sympathetic nerves. These effects can be modelled by: $C_v = C_{v0} - k_{C_v} N_s$, and $R_s = R_{s0} + k_{R_S} N_s$.

The model described in this paper is a beat-to-beat one. For this reason, the outputs of the controller have been discretized as follows:

$$\begin{aligned} T^*(t) &= T(t_i) \ , \ \forall t \in [t_i \ , \ t_{i+1}[\\ I^*(t) &= I(t_i) \ , \ \forall t \in [t_i \ , \ t_{i+1}[\end{aligned}$$

with $t_{i+1} = t_i + T(t_i)$, and $T(t) = \frac{60}{HR(t)}$ is the cardiac period.

D. The electro-chemical command

The circulation of blood is due to the contractions of the ventricles controlled by changes in calcium concentration inside the contractile cells. The myosin heads can attach to the actin molecules only if the binding sites are accessible which necessitates the presence of calcium on the tropomyosin [19], [20], [21].

For our purpose, it will be sufficient to use the approximate representation of the intracellular calcium concentration C_i during twitch transients given by [21]:

$$C_i(t) = C_{a_0} + (C_{a_{max}} - C_{a_0}) \frac{t}{\tau_{Ca}} \exp(1 - t/\tau_{Ca}) \tag{15}$$

It has a resting level $C_{a_0} = 0.01 \mu M$ and achieves its maximum value $C_{a_{max}} = 1 \mu M$ at time $\tau_{Ca} = 0.06s$.

The dynamic of binding of the intracellular calcium on tropomyosin is modelled as follows [11]:

$$\left\{ \begin{array}{ll} \dot{C}_T & = -k_{on} C_i C_T + k_{off} C_{TCa} \\ \dot{C}_{TCa} & = k_{on} C_i C_T - k_{off} C_{TCa} \end{array} \right. \tag{16}$$

where C_T is the concentration of free tropomyosin and C_{TCa} is the concentration of calcium bound up with tropomyosin.

The total tropomyosin concentration, $C_{TO} = C_T + C_{TCa}$ is constant and the fraction of occupied tropomyosin sites, $\theta_{TCa} = \frac{C_{TCa}}{C_{TO}}$ is solution of:

$$\dot{\theta}_{TCa} = k_{on} C_i (1 - \theta_{TCa}) - k_{off} \theta_{TCa} \tag{17}$$

In order to link θ_{TCa} to the input u of the muscle model (1)...(4), we consider that the contraction starts when $\theta_{TCa} \geq \theta_0$, corresponding in steady state to $C_i \geq \bar{C} = \frac{k_{off}}{k_{on}} \frac{\theta_0}{1 - \theta_0}$ and we take u as a piecewise linear function of $\theta_{TCa} - \theta_0$:

$$u = \left\{ \begin{array}{l} k_+(\theta_{TCa} - \theta_0) \ \text{ if } \ \theta_{TCa} \geq \theta_0 \\ k_-(\theta_{TCa} - \theta_0) \ \text{ if } \ \theta_0 > \theta_{TCa} \geq \theta_{00} \\ 0 \ \text{ if } \ \theta_{00} > \theta_{TCa} \end{array} \right. \tag{18}$$

We have $0 \leq \theta_{TCa} \leq 1$ and $-k_- \theta_0 \leq u \leq k_+(1 - \theta_0)$. If (17) is fast enough, $\theta_{TCa} = \frac{k_{on} C_i}{k_{on} C_i + k_{off}}$.

The contractility increases with θ_{TCa} and then with C_i, so that we take $C_{a_{max}}$ as the inotropy control I.

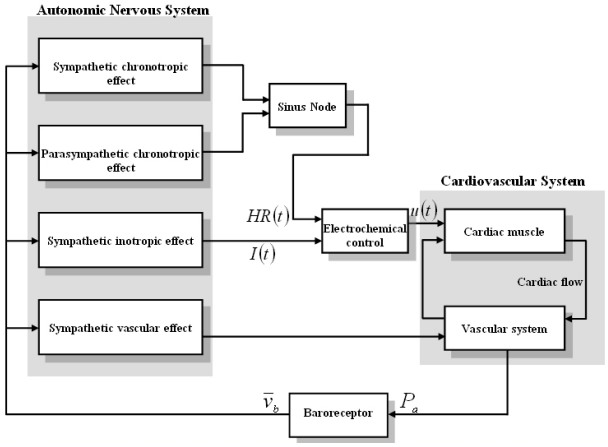

Fig. 2. Closed loop diagram of the cardiovascular system control.

Calcium uptake during active relaxation is modelled by k_- and k_{off} similar to the gain of a calcium pump in (17).

For the simulations, we have taken: $\theta_0 = 0.5$, $k_{on} = 40 \mu M^{-1} s^{-1}$ and $k_{off} = 20 s^{-1}$ so that $C_i \geq \frac{k_{off}}{k_{on}} = 0.5 \mu M$; $\theta_{00} = 0.2$, $k_+ = 200 s^{-1}$ and $k_- = 100 s^{-1}$.

III. ORTHOSTATIC TILT TEST

The main hemodynamic change due to the transition from supine to standing, is the redistribution of the venous blood volume, from the intrathoracic region towards the venous volume in the legs and the lower abdominal veins. The venous system is relatively very distensible; so the very large increase in transmural pressures (the difference between pressure inside and outside the veins) in the lower limbs will increase a lot their capacity. Immediately after standing, or being tilted, much of the flow of blood emerging from the capillary bed into these veins will remain there to fill the veins and to increase their capacity, instead of flowing on back to the heart. Thus, immediately after standing, there is a temporary decrease of venous return to the heart, until the venous reservoir is filled under the new transmural pressure, and then a steady state is reached and venous return will be as large as before. The control system increases heart rate, cardiac contractility and vascular tone by a decrease of vagal outflow and an increase of sympathetic outflow.

In the present model, only the venous compliance is affected because it depends of the transmural pressure and therefore of the term due to the gravity, so that

$$C_v(P_v) = C_{v0} - k_{C_v} N_s + c_v P_v \tag{19}$$

where c_v is the pressure sensitivity of the compliance.

An approximate solution of (9), (19) is

$$\begin{array}{l} P_v = \frac{1}{C_v(\theta)} [V_t - C_a P_a - V_{lv}] + \rho g h_v \sin\theta \\ \texttt{with } C_v(\theta) = C_{v0} - k_{C_v} N_s + c_v \rho g h_v \sin\theta \end{array} \tag{20}$$

During the orthostatic tilt test ($\triangle t_{tilt} = 5s$), it is assumed that $\theta(t) = a_\theta (t - t_{tilt})$, with $\theta \in [0, \frac{\pi}{2}]$, and $a_\theta = \frac{\pi}{10}$

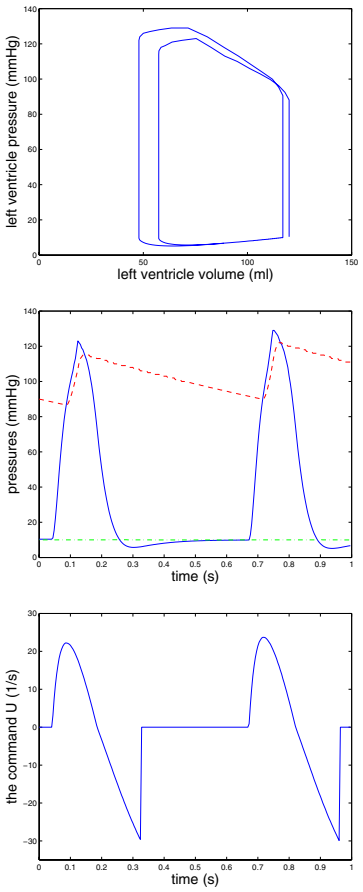

Fig. 3. Top: left ventricle pressure/volume function during two basal cardiac cycles. Middle: time pattern of left ventricle pressure (continuous line), arterial pressure (dashed line) and venous pressure (dot-dashed line). Bottom: time pattern of the command u.

IV. RESULTS

Numerical integration of differential equations was performed using the fifth-order Runge-Kutta-Fehlberg method with the software package SCILAB/SCICOS devoted to the simulation of ordinary differential equations.

The simulated time patterns of some hemodynamic quantities (arterial pressure, venous pressure, left ventricle pressure and the electro-chemical command) are shown in the middle and bottom panels of figure 3. In simulation, the state variables have the desired qualitative evolution. For each cardiac cycle, the rise of u is followed by the rise in the left ventricle pressure, as long as this pressure is lower than the arterial pressure and the volume remains constant. After that, the ejection starts (the left ventricular volume decreases). Then u becomes negative and the ventricular pressure brutally decreases, implying the aortic valve closing. From this moment, the ventricular volume is constant again. When the pressure becomes lower than that in the veins, the filling starts until the ventricular pressure becomes equal to the venous pressure, which implying the mitral valve closing. A new cycle can then begin.

Many studies investigated the aspect of cardiovascular

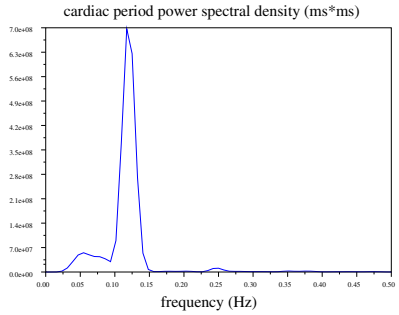

Fig. 4. Spectral analysis of simultaneous cardiac period variability.

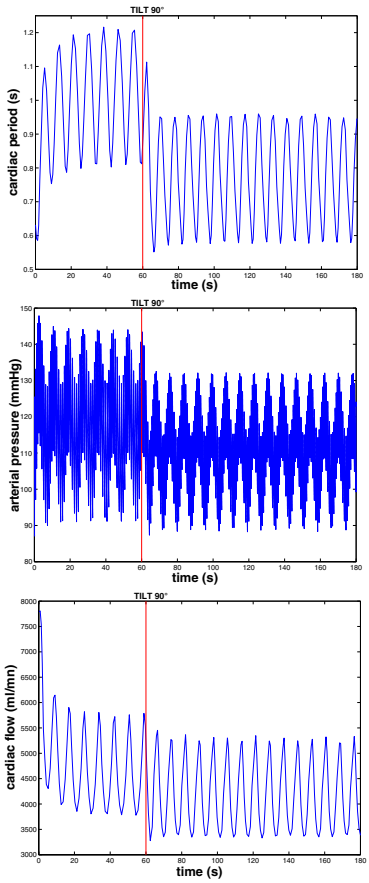

Fig. 5. Cardiovascular signals in a tilt up test. Top: time pattern of the cardiac period. Middle: time pattern of the arterial pressure. Bottom: time pattern of the cardiac flow.

variability with specific attention of the role of the baroreceptor [2]. The baroreflex acts as a nonlinear negative-feedback. In human, baroreflex changes of heart activity start after at least 0.5 s and the control action is fulfilled with a 2 s time delay. It is well known that nonlinear controls acting with a pure time delay can cause an oscillatory evolution [22]. The power spectrum analysis of cardiac period fluctuations is given (see figure 4). We recover the low frequency component, LF band (0.04-0.15 Hz), that is believed to be due to the baroreceptor mediated blood pressure and includes contributions from both sympathetic and parasympathetic nervous systems [3].

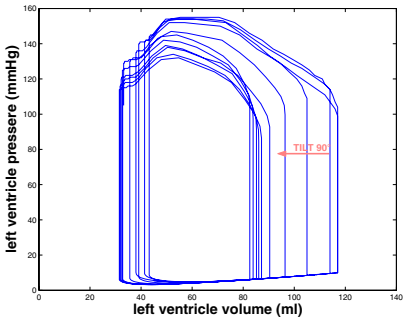

Fig. 6. Left ventricle pressure/volume function in a tilt up test.

The spectral analysis of heart rate variability can quantify graded changes in sympathovagal balance induced by passive tilt. The current opinion is that the slight tachycardia usually accompanying upright position is the result of a sympathetic excitation associated to a vagal withdrawal in the neural modulation of sinus node pacemaker activity [23], [24]. The heart rate simulation reproduces the general trend of the experimental finding (top panel of figure 5). Arterial pressure and cardiac flow simulations present a bias (middle and bottom panels of figure 5) which is assumed to be due to the distance of the baroreceptor from the hydrostatic indifference point, where we suppose that the pressure is regulated, we observe that the pressure at the point h_a lower than the baroreceptor position is without bias. The effects of variable filling and ejection conditions during the tilt test is shown in figure 6.

V. CONCLUSION

The aim of this paper was to propose a model simple enough to be further studied and able to reproduce some experimental results about short term control of the cardiovascular system (the process) by the autonomic nervous system (the controller) corresponding to the physiological conditions and to the hemodynamic perturbation (graded tilt test). The proposed model, based on previous models of cardiovascular sub-systems, has 6 state-variables for the process and 4 for the controller. It has been possible to tune the controller with realistic parameters in order to recover the main phenomena observed during an orthostatic stress. In particular, the similitude of the results of the short-term spectral analysis of the heart rate variability confirm the role of the sympathovagal balance, the main feedback considered here. This kind of model may help to define and identify clinical indexes from heart rate and pressure measurements.

REFERENCES

[1] W. H. Levison, G. O. Barnett, and W. D. Jackson, "Nonlinear analysis of the baroreceptor reflex system," *Circulation Research*, vol. XVIII, pp. 673–682, 1966.

[2] H. Seidel and H. Herzel, "Modelling heart rate variability due to respiration and baroreflex," *Springer Series in Synergetics*, vol. 65, pp. 205–229, 1995.

[3] S. Cavalcanti and E. Belardinelli, "Modeling of cardiovascular variability using a differential delay equation," *IEEE Transactions on Biomedical Engineering*, vol. 43, no. 10, pp. 982–989, 1996.

[4] F. Kappel and R. O. Peer, "a mathematical model for fundamental regulation processes in the cardiovascular system," *J. Math. Biol.*, vol. 31, pp. 611–631, 1993.

[5] M. Ursino, "Interaction between carotid baroregulation and the pulsating heart: a mathematical model," *Am. J. Physiol*, vol. 44, pp. H1733–H1747, 1998.

[6] A. Monti, C. Médigue, and M. Sorine, "Short-term modelling of the controlled cardiovascular system," in *Modelling and Simulation for Computer-aided Medicine and Surgery(MS4CMS)*, E. Proceedings, Ed., vol. 12, 2002, pp. 115–128.

[7] J. Bestel and M. Sorine, "A differential model of muscle contraction and applications," in *Schloessmann Seminar on Mathematical Models in Biology, Chemistry and Physics*, Max Plank Society, Bad Lausick, Germany, May 2000.

[8] J. Bestel, F. Clément, and M. Sorine, "A biomechanical model of muscle contraction," in *Lectures Notes in Computer Science*, vol. 2208. Eds W.J. Niessen and M.A. Viergever, Springer-Verlag, 2001, pp. 1159–1161.

[9] L. Amaral, A. Goldberger, P. Ivanov, and H. Stanley, "Modeling heart rate variability by stochastic feedback," *Computer Physics Communications*, vol. 121-122, pp. 126–128, 1999.

[10] A. Monti and M. Sorine, "Baroreceptor modelling and a possible role of the sympathetic efferent activity," in *Minisymposium on Innovative approaches to mathematical modeling of biomedical systems*, ser. ECMTB2002 - European Conference for Mathematical and Theoretical Biology, Milan, Italy, July 2002.

[11] J. J. Rice, R. L. Winslow, and C. W. Hunter, "Comparison of putative cooperative mechanisms in cardiac muscle: length dependence and dynamic responses," *Am J Physiol Heart Circ Physiol*, vol. 276, no. 5, pp. H1734–1754, 1999.

[12] D. M. Bers, "Cardiac excitation-contraction coupling," *Nature*, vol. 415, no. 6868, pp. 198–205, 2002.

[13] T. Heldt, E. Shim, R. Kamm, and R. Mark, "Computational modeling of cardiovascular response to orthostatic stress," *J Appl Physiol*, vol. 92, pp. 1239–1254, 2002.

[14] Kubota, T., H. Chishaki, T. Yoshida, K. Sunagawa, A. Takeshita, and Y. Nose, "How to encode arterial pressure into carotid sinus nerve to invoke natural baroreflex," *Am. J. Physiol (Heart Circ. Physiol.)*, vol. 263(32), pp. H307–H313, 1992.

[15] H. R. Warner, "The frequency-dependent nature of blood pressure regulation by the carotid sinus studied with an electric analog," *Circulation Research*, vol. 6, pp. 35–40, 1958.

[16] D. Boer, Karemaker, and Strackee, "Hemodynamic fluctuations and baroreflex sensitivity in humans: Beat-to-beat model," *Am. J. Physiol (Heart Circ. Physiol)*, vol. 253(22), pp. 680–689, 1987.

[17] Katona, "Sympathetic and parasympathetic cardiac control in athletes and nonathlete at rest," *J. App. Phyiol: Respirat. Environ. Exercise Physiol*, vol. 52, no. 6, pp. 1652–1657, 1982.

[18] Warner and Cox, "a mathematical model of the heart rate control by sympathetic and vagus efferent information," *J. App. Phyiol*, vol. 17, pp. 349–355, 1962.

[19] V. Novak and J. Neumann, "Mathematical model of the electromechanical heart contractile system - simulation results," *I. J. of Bioelectromagnetism*, vol. 2, no. 2, 2000.

[20] M. Mlcek, J. Neumann, O. Kittnar, and V. Novak, "Mathematical model of the electromechanical heart contractile system - regulatory subsystem physiological consideration," *Physiological Research*, vol. 50, pp. 425–432, 2001.

[21] P. Hunter, A. D. McCulloch, and H. ter Keurs, "Modelling the mechanical properties of cardiac muscle," *Progress in Biophysics & Molecular Biology*, vol. 69, pp. 289–331, 1998.

[22] M. Akian, P.-A. Bliman, and M. Sorine, "Control of delay systems with relay," *IMA Journal on Mathematical Control and Information, Special issue on analysis and design of delay and propagation systems*, vol. 19, no. 1 & 2, Special Issue, 2002.

[23] S. Jasson, C. Médigue, P. Maison-Blanche, N. Montano, L. Meyer, C. Vermeiren, P. Mansier, P. Coumel, A. Malliani, and B. Swynghedauw, "Instant power spectrum analysis of heart rate variability during orthostatic tilt using a time-frequency domain method," *Circulation*, vol. 96, pp. 3521–3526, 1997.

[24] N. Montano, T. G. Ruscone, A. Porta, F. Lombardi, M. Pagani, and A. Malliani, "Power spectrum analysis of heart rate variability to assess the changes in sympathovagal balance during graded orthostatic tilt," *Circulation Research*, vol. 90, no. 4, pp. 1826–1831, 1994.